RAPID MAGNETICALLY-GUIDED ATTRACTION OF SPION-LADEN HUVEC TO MAGNETIC STEEL SURFACE

Paulina Trzaskowska[1]*, Ewa Rybak[1], Jakub Krzemiński[1], Dominik Baraniecki[1], Iwona Cicha[2]

[1] Warsaw University of Technology, Centre for Advanced Materials and Technologies, Poleczki 19, 02-781 Warsaw, Poland
[2] Section of Experimental Oncology und Nanomedicine (SEON), Else Kröner-Fresenius-Stiftung-Professorship, ENT-Department, Universitätsklinikum, GluckstraBe 10a, Erlangen 91054, Germany
*e-mail: paulina.trzaskowska@pw.edu.pl

Abstract

Steel has been extensively utilized in vascular implants due to its mechanical strength, corrosion resistance, and clinical reliability. However, concerns regarding thrombogenicity and vascular injury have limited its long-term performance. A critical factor for the success of metallic implants is endothelialization, which prevents thrombosis, restenosis, and promotes implant integration. This study explores the use of endothelial cells (HUVECs) laden with superparamagnetic iron oxide nanoparticles (SPION) to culture on magnetic stainless steel (MS) surfaces. The objective was to investigate the effect of a weak magnetic field generated by MS on HUVEC attraction, comparing it with non-magnetic stainless steel (SS) and SS with an external neodymium magnet under static and flow culture conditions. The results demonstrated that MS surfaces, influenced by SPION, facilitated significantly improved HUVEC adhesion and focal adhesion point formation compared to SS and SS with an external magnet. Profilometric analysis revealed sharper topographical features on MS surfaces, which, despite their roughness, did not hinder cellular adhesion but instead promoted cell spreading and increased focal adhesion strength. Under static conditions, MS surfaces exhibited enhanced cytoskeletal remodelling and stronger focal adhesion formation. However, under flow conditions, the benefits were less pronounced, indicating the need for further optimization of surface features and magnetic properties to improve endothelial retention in dynamic environments. This research provides valuable insights into SPION-mediated endothelialization for magnetic stainless steel implants, highlighting their potential for enhancing biocompatibility and long-term performance in vascular applications. Further optimization is necessary to fully realize their potential in dynamic physiological settings.

Keywords: *endothelialization, HUVEC, steel, vascular implants*

[Engineering of Biomaterials 172 (2024) 11]

doi:10.34821/eng.biomat.172.2024.11

Submitted: 2024-11-20, Accepted: 2024-12-18, Published: 2024-12-22

Introduction

Stainless steel has been widely used in vascular implants due to its mechanical strength, corrosion resistance, and clinical reliability. The introduction of self-expandable stainless steel mesh stents by Sigwart et al. [1] marked a significant advancement in cardiovascular interventions by preventing arterial occlusion and restenosis. Subsequent studies have demonstrated that intracoronary stents improved procedural safety and success rates compared to balloon angioplasty alone [2]. However, concerns regarding thrombogenicity and vascular injury associated with bare-metal stainless steel stents have also been reported [3]. Despite these challenges, advancements in material engineering, such as surface modifications and drug-eluting coatings, have significantly improved the biocompatibility and long-term performance of stainless steel stents [4].

A critical factor in the success of metallic vascular implants is endothelialization, which is essential for reducing complications such as thrombosis and restenosis. The presence of an intact viable endothelial layer minimizes platelet adhesion and activation, thereby preventing thrombotic events [5]. Additionally, endothelial coverage plays a crucial role in moderating inflammatory responses, inhibiting smooth muscle proliferation, and promoting implant integration through enhanced endothelial progenitor cell attachment [6]. Therefore, strategies aimed at improving endothelialization on the metallic implants surface have become a focal point in the development of next-generation stainless steel implants. Recent studies have explored various endothelialization strategies, including biomimetic coatings, antibody-based capture, and nanoparticle-mediated targeting. Biomimetic coatings, such as self-assembled peptide nanofibers and mussel adhesive mimics, have been shown to significantly enhance endothelial cell (EC) adhesion and proliferation [5,7]. Antibody-based methods utilizing anti-CD34 and anti-VEGFR2 have demonstrated improved EC capture and retention [8].

Meanwhile, the use of magnetic nanoparticles (MNPs) has emerged as a promising approach for guiding EC to implant surfaces, achieving high rates of endothelial coverage *in vitro* and *in vivo*. Various EC types, such as human umbilical vein, bovine aortic, and endothelial progenitor cells, have been loaded with MNPs through direct incubation, pre-labeling, and endocytosis. These methods achieved high cell viability and complete nanoparticle uptake within 24 hours [9,10]. MNPs-based strategies further supported the endothelialization of the metal surfaces.

In this research, we evaluated the process of SPION-mediated targeted attraction of HUVEC to the surface of magnetic steel (MS), producing a weak magnetic field, and compared it to HUVEC adhesion to non-magnetic steel and non-magnetic steel in the presence of a neodymium magnet. The objective of this study was to examine the possibility of obtaining strong HUVEC adhesion on MS in a short-time culture (30 min or 2 h) and to investigate whether the magnetic field provided by MS still enhances cell attraction and focal adhesion points formation during both static and flow cell culture.

Materials and Methods

Steel materials magnetization

Two types of steel discs (ϕ 14 mm) and slabs (35 x 5 mm) made of stainless steel 316 L (1.4404, labelled as SS) and H17 ferritic magnetic steel (1.4016, labelled as MS) were used. Both types of steel were provided by Stomilex Sp. z o.o. (Poland). Fe content declared by the producer equals 63-66% in SS and 77-81% in MS. Before any tests, in order to permanently arrange magnetic domains, the MS samples were magnetized with the use of a round neodymium magnet (ϕ 15 mm) with surface magnetic flux of 500 mT. The magnet was simply stuck vertically to the flat surface of a disc or the middle of a slab for 1 s. The magnetic field strength obtained for the steels was then measured with a magnetometer (FM 302 Teslameter equipped with transverse probe AS-NTM, Elektronik GmbH Berlin).

Profilometric imaging of SS and MS surface

Surface topographical scanning and surface roughness measurement in five separate locations were performed with a DektakXT stylus profilometer from Bruker with the NLite + package. A tip with a radius of 2 μm was used, and the measured length was 1.8 mm. The results were analysed using the vision64 software from Bruker.

SPION synthesis and characterization

Lauric acid-coated iron oxide superparamagnetic nanoparticles (SPION) were synthesized as described in previous works by the co-precipitation method [11]. Fe (II) and Fe (III) salts (3:2 molar ratio) were dissolved in water, precipitated with NH_3, and washed with 1.3% of ammonium hydroxide. Lauric acid was then added, and the mixture was heated to 90°C for 4 min under stirring. The resulting lauric acid-coated particles were washed 10 times with 1.3% of ammonium hydroxide solution.

The iron content in SPION was established previously and given in the Results section. Briefly, the particles were diluted 1:100 and dissolved in HCl at 90°C. After being cooled to room temperature, 10% hydroxylammonium chloride solution, sulfosalicylic acid, and NH_3 were added. The iron content was then determined by measuring the ultraviolet (UV) absorbance at 405 nm with a microplate reader (Filtermax F5; Molecular Devices, Sunnyvale, CA, USA) [11]. In addition, magnetization curves were measured with the application of a vibrating sample magnetometer (VSM) [12].

The average particle sizes and polydispersity index (PDI) were measured through dynamic light scattering (DLS) using the Malvern Zetasizer (Nano ZS, Malvern Instruments, Malvern, UK), equipped with a detector to measure the intensity of the scattered light at 173◦ to the incident beam. The suspension of iron oxide nanoparticles was diluted 500 times in ultrapure water. Surface charge measurements characterized by the zeta potential (ζ), were conducted in ultrapure water with 0.1M PBS buffer (pH 7.4) in a 9:1 volume ratio. All measurements were made in triplicate to ensure reproducibility.

Cytotoxicity of steel samples

The MTT assay (Thiazolyl Blue Tetrazolium Bromide, Sigma Aldrich) was conducted to assess the cytotoxicity of steel samples. Mouse fibroblasts L929 (Sigma Aldrich) were harvested and resuspended in supplemented DMEM medium (with 10% of FBS, 2 nM of L-glutamine, 100 units/ml of penicillin and 100 μg/ml of streptomycin), seeded in a 96-well plate at 10^4 cells/100 μl and incubated for 24 h. Meanwhile, according to ISO 10993-5 and 10993-12 standards, extracts were prepared in triplicate for both SS and MS by incubation in a supplemented DMEM medium w/o Phenol Red (1 ml per 3 cm^2 of disc surface) for 24 h (37ºC, 5% CO_2).

After extraction, the extracts were filtered and added to the cells for subsequent 24 h of incubation. As a negative and positive control (NC and PC, respectively), DMEM medium w/o Phenol Red (NC) and DMEM medium w/o Phenol Red with 0.1% (v/v) of Triton X (Sigma Aldrich) (PC) were used. Then, extracts were discarded from the wells, and MTT solution (1 mg/mL in DMEM w/o Phenol Red) was added. Formazan crystals were dissolved after 4 h with 10% of SDS. The optical density (OD) of the solutions was detected at 570 nm (Spectramax iD3, Molecular Devices). Each extract was measured six times. The cytotoxicity results were presented as % NC.

HUVEC culture and SPION loading

Human umbilical vein endothelial cells (HUVECs) were isolated from freshly collected umbilical cords (courtesy of the Department of Gynaecology, University Hospital Erlangen) using a standard technique. The use of human material was approved by the local ethics committee of the University Hospital Erlangen. Cells were maintained in Endothelial Cell Growth Medium (ECGM, PromoCell, Heidelberg, Germany) supplemented with 5% of foetal calf serum, 4 μL/mL of heparin, 10 ng/mL of epidermal growth factor, 1 μg/mL of hydrocortisone, 50 μg/mL of gentamycin sulphate, and 50 ng/mL of amphotericin B, under a humidified 5% CO_2 atmosphere. All experiments were conducted using HUVECs at passages 1–2.

Confluent HUVECs were pre-incubated with SPION suspension obtained as described above in 75 cm^2 cell culture flasks. In particular, 15 μl of SPION stock solution (14.22 mg/ml) was added to 10 ml of complete HUVEC culture medium, gently mixed, and then medium with SPION was added to confluent HUVEC cells adhered to the bottom of the flask. The final amount of Fe coming from, SPION in medium was 3 μg Fe/cm^2. Cells were incubated with SPION at 37°C, 5% CO_2 for 16 h to enable endocytosis. The used concentrations had been selected based on the previously reported dose-finding studies, according to which, such an amount is not considered cytotoxic (HUVEC viability ≥ 75%) [11]. The iron concentration per cell quantified with microwave plasma atomic emission spectroscopy (MP-AES, 4200 device, Agilent) was 0.0247 ng/cell.

Outline of the cell cultures setup

FIG. 1 shows the schematic workflow of the HUVEC cultures.

SPION-loaded HUVECs were cultured statically with SS, MS, and SS with a magnet in order to provide a comparison for cells attraction to MS presenting a weak magnetic field. For flow culture, SPION-loaded HUVECs were subjected to SS and MS slabs.

HUVECs without SPION were also applied for adhesion on SS, MS, and SS with a magnet in static conditions to evaluate the effect on the surface alone on the cells. The following paragraphs describe the HUVECs cultures in detail.

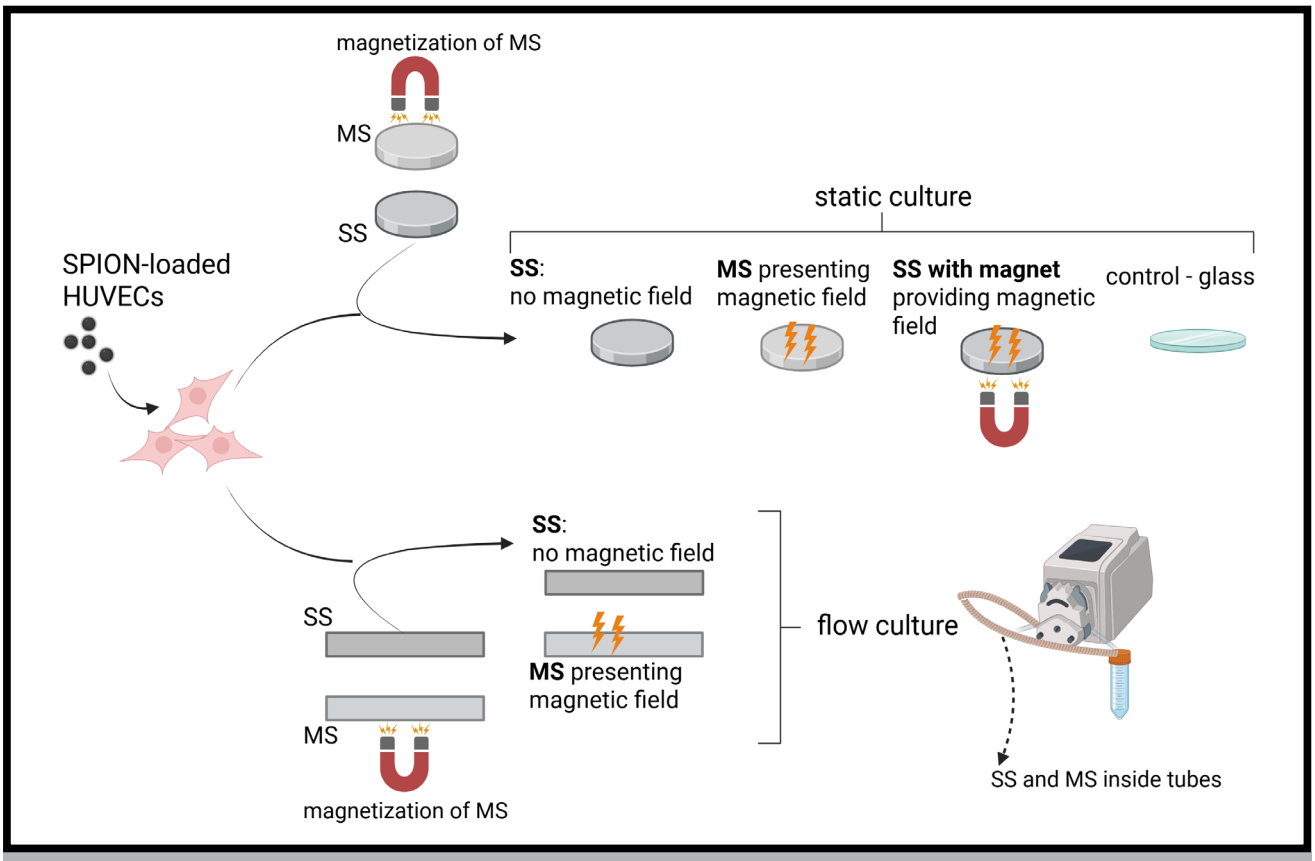

FIG. 1. Scheme of the present research workflow. Created in BioRender. Trzaskowska, P. (2025) https://BioRender.com/remg3lv.

Static and flow culture of HUVECs with SPION on steel samples

For static HUVEC culture, steel discs were applied, whereas for flow culture, steel slabs were used. First, the SS and MS materials were sterilized in 70% of EtOH for 30 min. After that, the samples were rinsed with a sterile buffer solution, Dulbecco's phosphate buffered saline (DPBS), three times under the laminar hood. For static culture, the discs were placed in the fresh 24-well plate, and for flow culture, the slabs were kept in sterile DPBS in centrifuge tubes.

The SPION-loaded cells were harvested and centrifuged, followed by cell counting.

For static culture, SPION-laden HUVECs were suspended in a culture medium and transferred onto the steel discs (in triplicates) in a 24-well plate ($1x10^5$ cells/ml). In the case of samples labelled 'SS with magnet' a round neodymium magnet (500 mT) was kept underneath the well through the culture period. MS samples were magnetized as described above, whereas SS samples did not present a magnetic field. The cells were allowed to adhere on the samples surface for 30 min and 2 h. After that time, the materials were gently rinsed with PBS, fixed with 4% (v/v) paraformaldehyde (PFA) and stained with fluorescent dyes (see below). Glass cover slides were used as control materials of cells adhesion.

For flow culture, SPION-laden HUVECs as described above were suspended in the culture medium at $2.5x10^5$ cells/ml to mimic the arterial flow conditions. The flow system was assembled in sterile conditions as described before [13]. Peristaltic pump (model Ismatec IPC 8, Idex, Wertheim, Germany) was used. The slabs (MS magnetized as described above, SS not showing any magnetic field) were placed in 3 cm long, 4.8 mm diameter sterile ismaprene tubes (PharMed, Idex) in triplicates, connected sequentially using Luer-Luer connectors. The shear stress of 10 dyne/cm^2 for 20 h was applied, at 37ºC and 5% CO_2. The substrates were subsequently washed DPBS, removed from the tubes, placed in centrifuge tubes, fixed with 4% (v/v) of PFA and stained with fluorescent dyes (see below). FIG. 2 shows the schematic illustration of the flow culture system.

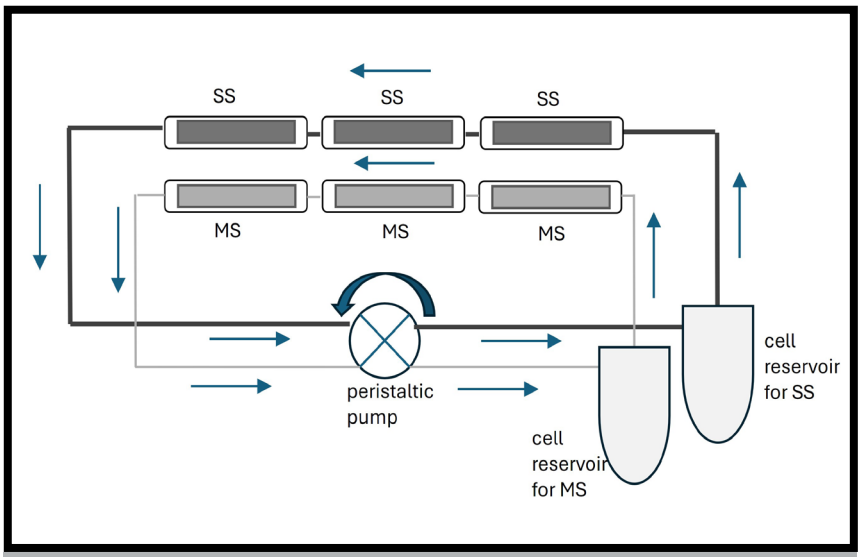

FIG. 2. Schematic illustration of the flow culture system applied for SPION-laden HUVEC adhesion on SS and MS.

Static culture of HUVEC without SPION on steel discs

In order to check the effect of surface alone on cells attachment, HUVEC without SPION were also subjected to attachment on SS and MS discs. The samples were sterilized as described above. The HUVECs were seeded on the discs in a 24-well plate ($1x10^5$ cells/ml) and were let to adhere for 2 h and 24 h. After that, the cells were fixed and stained as described below. Glass cover slides were applied as controls.

Immunofluorescent staining of HUVECs on steel samples

The cells on SS and MS discs were fixed by 4% of PFA, permeabilized with 0.2% of Triton-X 100 and blocked with 1% of bovine serum albumin (BSA) in PBS. Samples from static culture with SPION-loaded HUVECs were then incubated with 1:200 CoraLite® Plus 488-conjugated FAK Monoclonal antibody (Proteintech) for 16 h, washed 3 times with PBS. Then, all samples were incubated with 1:400 CoraLite® 594-Phalloidin (Proteintech) at 37°C for 1 h, washed again with PBS, and finally nuclei were counterstained by 1:1000 DAPI (Thermofisher) for 10 min at room temperature. After washing with PBS, the discs were visualized using a fluorescence microscope Zeiss Axio Observer Z1 (Zeiss, Jena, Germany) at 20× magnification.

Analysis of fluorescent images

Cell counting on the fluorescence images was performed using the ImageJ software (version 1.47v). For HUVEC on discs after static culture, the following parameters were assessed: cell count, area occupied by cells, and circularity. All data were presented as mean ± standard deviation with a repetition of at least 5 times. Statistical analysis was performed by one-way analysis of variance (ANOVA) and Tukey's test, with significance reported when $p \leq 0.05$.

For HUVEC on slabs after flow culture, only imaging was performed.

Results and Discussions

Steel materials magnetization

The magnetic field strength of the MS samples was for discs from -0.4 to + 0.4 mT along the diameter and for slabs 1 mT in the middle and 0 mT at the edges. The magnetization of the MS samples was permanent, while the SS did not undergo any changes when affected by the magnets (magnetic field strength was 0 mT in every location on the SS surface).

Profilometric scans of SS and MS surface

3D scans of SS and MS samples obtained with an stylus profilometer revealed differences in the surface topography of SS and MS. SS was characterized with a less sharp profile with broader slopes. In contrast, MS surface shows parallel narrow scratches. This outcome is further proven by the measured value of kurtosis (Rku), which is the measure of the surface sharpness, which means that the higher the Rku, the sharper the slopes (Rku of SS = 6.407 µm, Rku of MS = 8.699 µm). What is important, the slopes on SS were higher closer to the edge (FIG. 3 b) than in the middle of the sample (FIG. 3 a). It might have been caused by the process of laser cutting of the elements. This effect was not so distinctive in the case of MS.

SPION characterization

The iron content for SPION was previously determined to be 14.22 mg/ml [12]. The superparamagnetic behaviour was also determined in the same work. The saturation magnetization MS calculated from magnetization curves was 174.80 A/m resulting in the volume fraction of magnetic material φ = 0.039% [12]

According to dynamic light scattering measurements, the average hydrodynamic diameter of SPION in distilled water was 46.97 ± 0.17 nm (FIG. 4) and their charge was negative (−19.00 ± 2.00 mV).

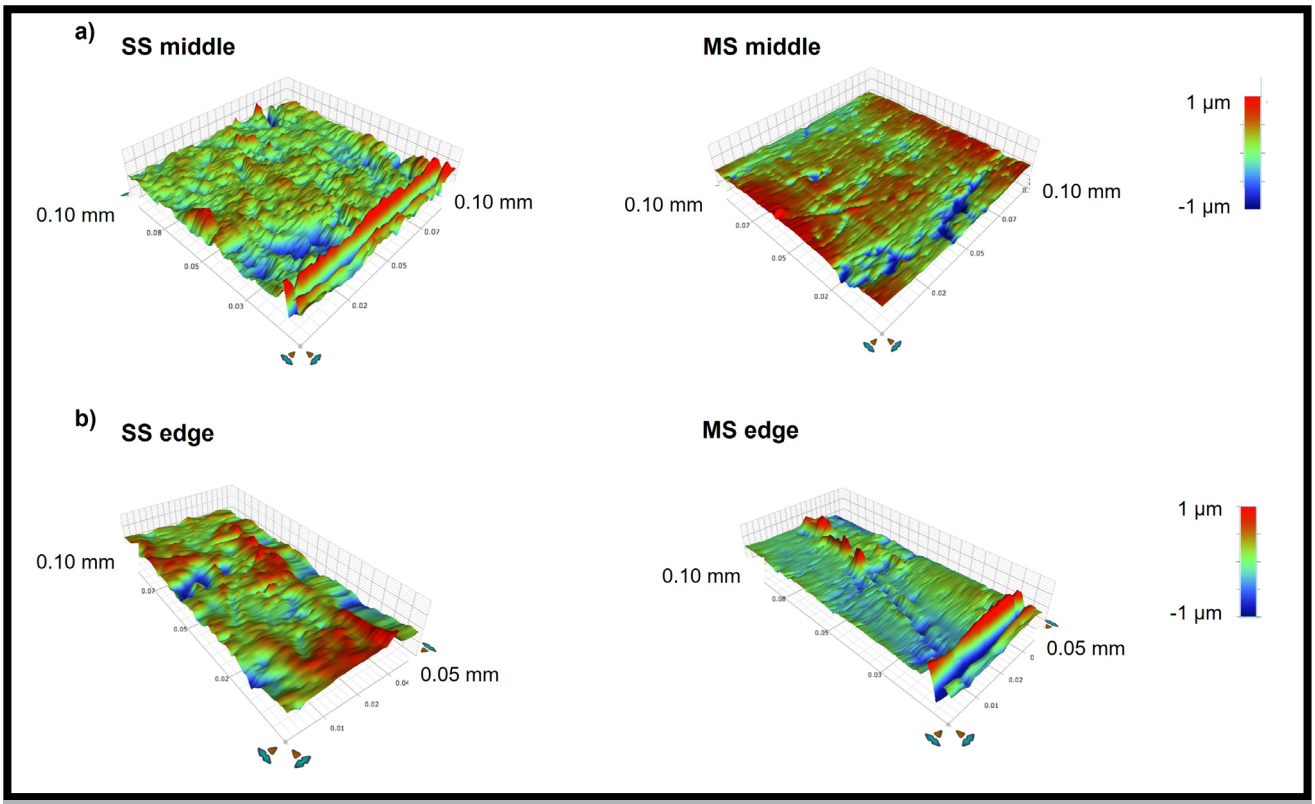

FIG. 3. 3D surface profiles of the SS and MS surfaces: a) in the middle of the samples, b) close to the edge of the samples.

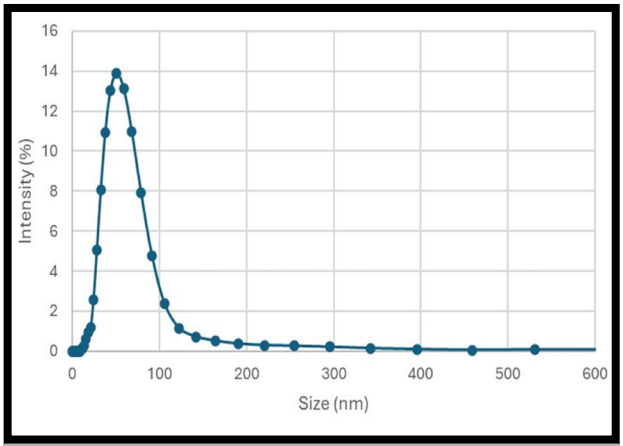

FIG. 4. Size distribution of SPION measured with DLS.

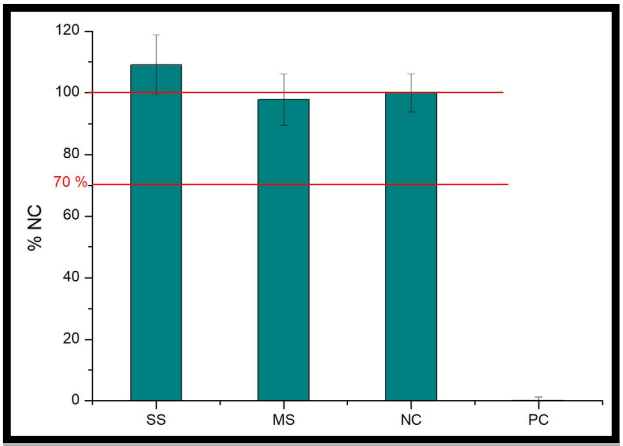

FIG. 5. MTT results for cytotoxicity of SS and MS samples.

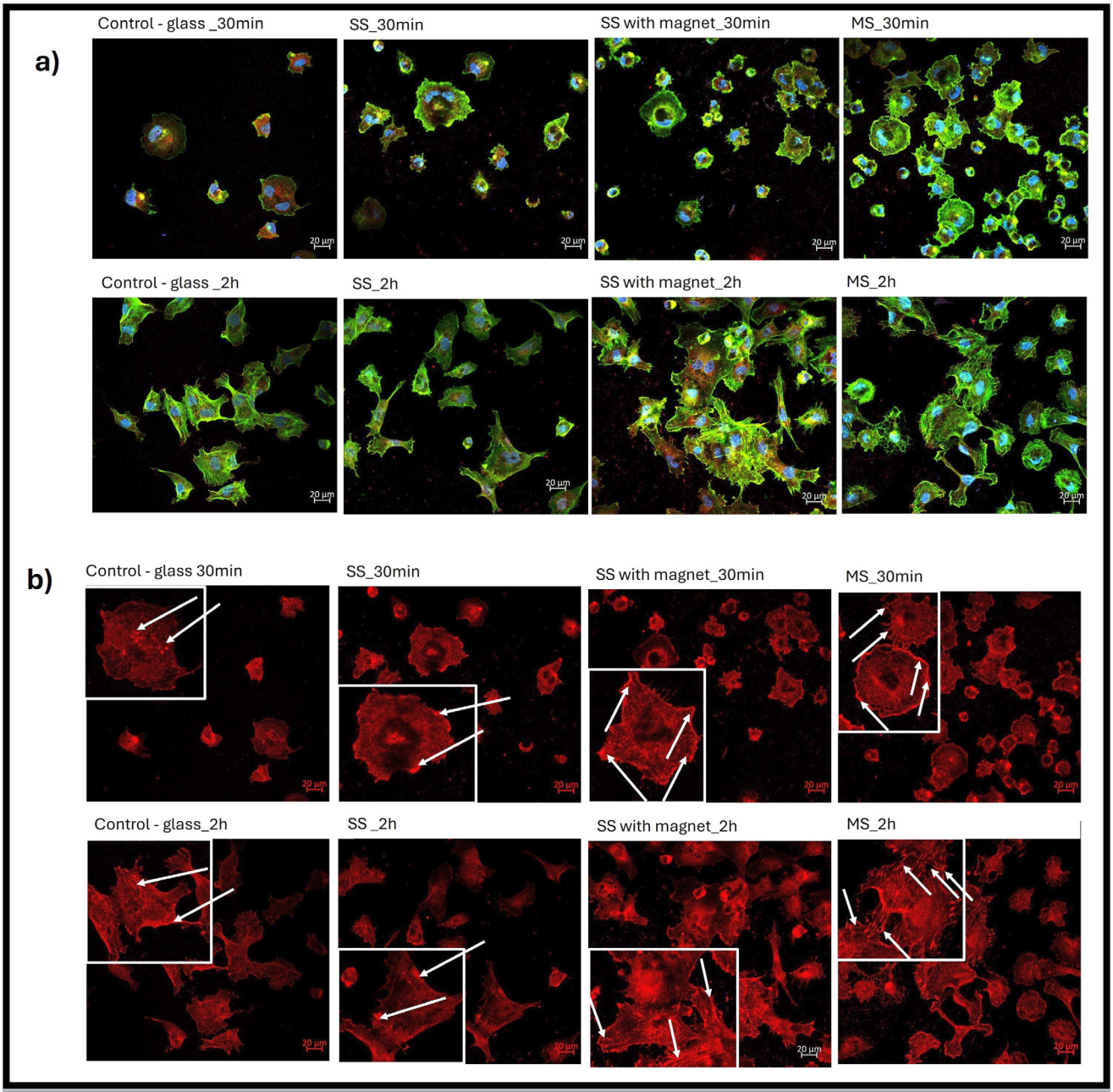

FIG. 6. Fluorescent images of SPION-loaded HUVECs adhered on steel samples: a) green – cytoskeleton, blue – nuclei, red – FAK, b) FAK alone. Selected enlarged cells are shown in the frames. Focal adhesion points are indicated by arrows.

Cytotoxicity of steel samples

According to the MTT assay, the SS and MS samples did not show cytotoxicity toward L929 cells, as the cell viability in contact with the extracts from the steels was near 100% with regard to the negative control (FIG. 5).

Visualisation and analysis of HUVECs on steel discs – static culture

The driving force required for the motility of eukaryotic cells is primarily produced by actin polymerisation. The conversion of force into cell movement is predominantly facilitated by focal adhesion points, defined as macromolecular multiprotein assemblies located at the extremities of actin fibres that serve to connect them to the extracellular matrix. The focal adhesion kinase (FAK) is a crucial protein for integrin-mediated focal adhesion point formation [14] and thus was utilised in the present study to evaluate the HUVECs-steel interaction.

As illustrated in FIG. 6, the FAK were observed to be concentrated at the extremities of the actin fibres, forming a band along the cell borders in HUVECs adhered to all samples (see arrows). This has previously been identified as a hallmark of strong adhesion and cellular motility [15]. However, for SS with magnet 2 h and especially MS 2 h, there are distinct FAK cluster alignments with the beginning and end of actin filaments (seen as enlarged bright points in FIG. 6 b). This finding suggests that the remodelling of the cytoskeleton is enhanced by the magnetic field, leading to an increased formation of focal adhesion points. This is a crucial process for maintaining a healthy endothelium [16].

For comparison, HUVEC without SPION adhered on steel samples were also visualised (FIG. 7). In contrast to the SPION-loaded HUVECs adhesion study, here, HUVECs appeared to have a cobblestone-like appearance, with actin filaments appearing straight and parallel through the cells.

FIG. 8 presents quantitative data obtained thanks to ImageJ analysis of fluorescence images of SPION-loaded HUVECs and HUVEC without SPION, respectively. The aim of this analysis was to find any statistically significant differences between results related to MS and every other material type. One star indicates significant differences in the calculated values between MS and other material variants at the first timepoint of culture, while two stars point out the significant differences between MS and other materials at the second timepoint.

Cell count is the most important outcome that determines the ability of the surface to attract SPION-loaded cells. The number of adherent HUVECs with SPION is the greatest on MS at each time point, and statistical significance was shown for MS and control (30 min and 2 h), and MS and SS (2 h). Despite no statistical significance, MS attracted more HUVECs than SS with a neodymium magnet, which has a 1000 times stronger magnetic field than MS. In the case of HUVECs without SPION, there were no significant differences in cell number.

The area occupied by cells did not vary significantly regardless of the presence of SPION. HUVECs laden with SPION covered most of the area on SS with magnet and on MS, demonstrating that magnetic field interaction with SPION affects cell spreading. This is particularly clear when compared to the control and the SS, both of which have no magnetic field.

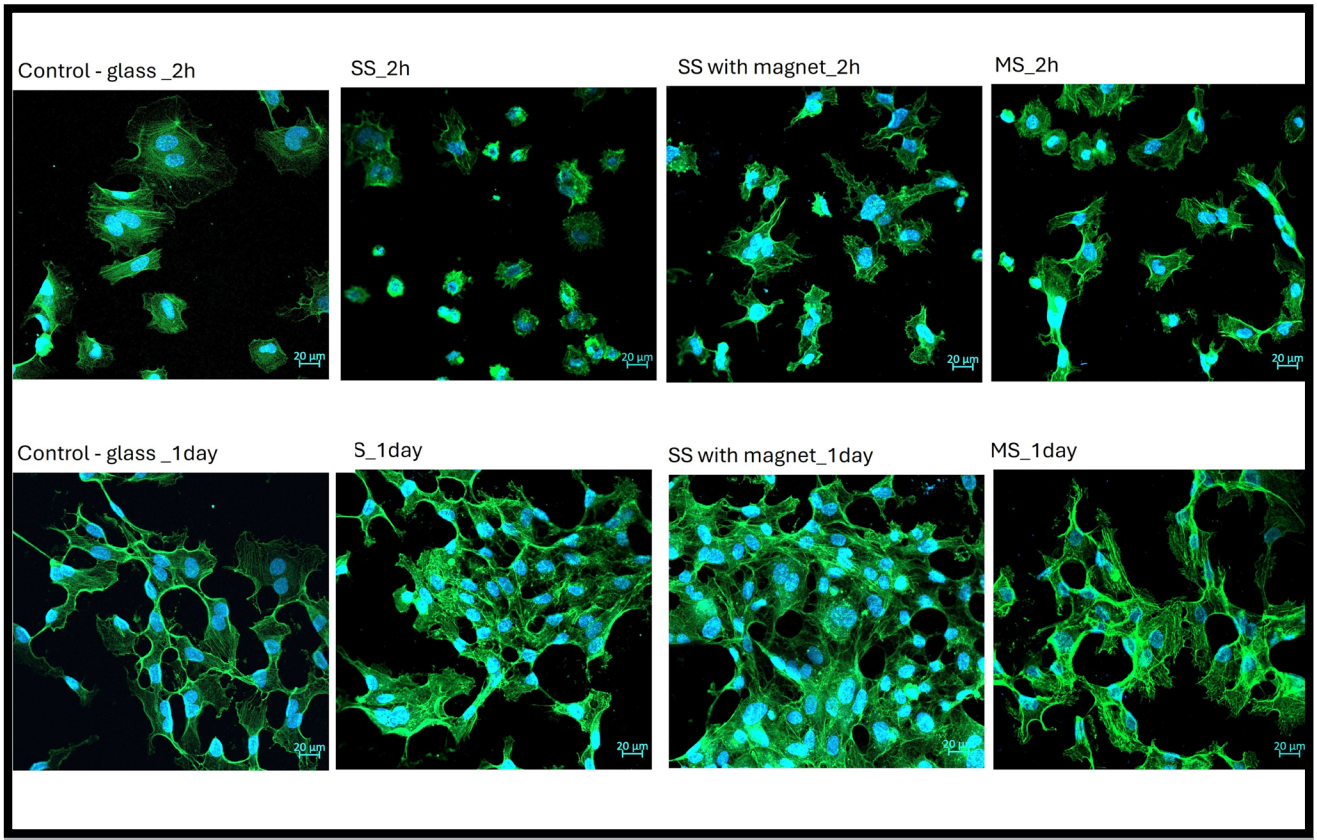

FIG. 7. Fluorescent images of HUVECs without SPION adhered on steel samples: green – cytoskeleton, blue – nuclei.

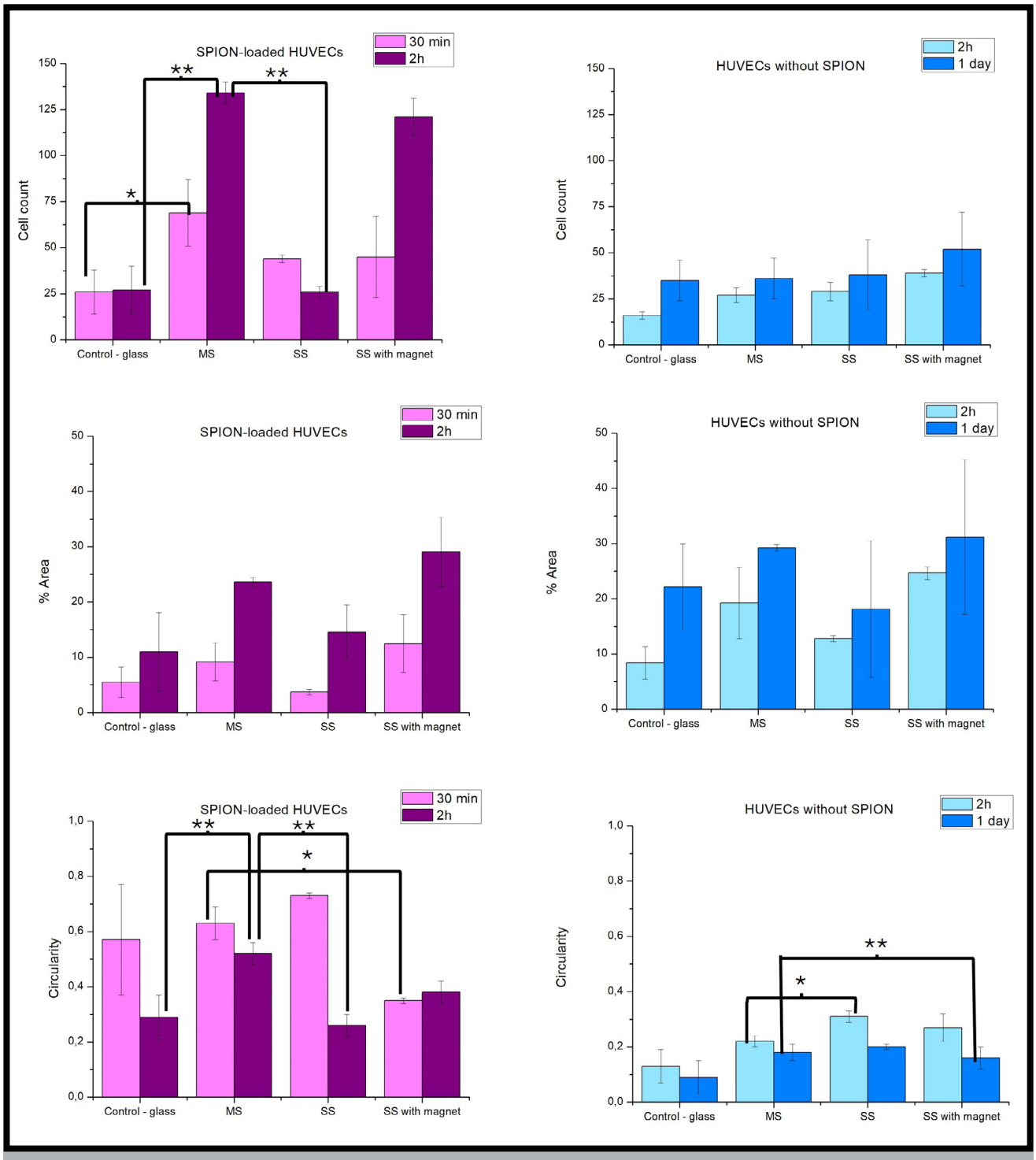

FIG. 8. Values of shape descriptors of cells calculated from confocal images of SPION-loaded HUVECs and HUVEC without SPION adhered of materials; statistical significances were indicated for the values obtained for MS; * - for the first timepoint of culture, ** - for the second timepoint; statistical analysis was performed by one-way analysis of variance (ANOVA) and Tukey's test, with significance reported when $p \leq 0.05$.

Circularity describes the roundness of the cells, which means that circularity value of 1.0 indicates a perfect circle. For glass control and SS, the circularity of SPION-loaded HUVECs decreases strongly, which may indicate elongation due to cell spreading along the scratches. In general, the circularity of SPION-loaded HUVECs is greater than that of SPION-free HUVECs at the same culture time (2 h) on the corresponding surfaces. The possible reason for this is that SPION uptake increase cell weight and thus pressure exerted on the steel surface. The smallest decrease in circularity of SPION-loaded HUVECs was observed at MS. For control and SS, the cells elongated significantly compared to MS. For SS with magnet, the circularity remained approximately the same. Generally, the circularity of SPION-loaded HUVECs after 2 h was the biggest on MS. This important outcome proves that magnetic interaction between SPION incorporated in the cells and the magnetic surface overcames the restricting effect of a sharp profile of MS on cells spreading.

The present study has revealed new insights into the matter, as such data for HUVECs have not been previously reported.

Visualisation of HUVEC on steel slabs – flow culture

Differences in profile topography depending on the location on th steel sample must have had affected the SPION-loaded HUVECs adhesion process during flow culture. FIG. 9 shows the stained HUVECs located in different spots on the materials surface. It can be concluded that higher slopes present closer to the edges of SS trapped HUVECs and prevented the detachment, in contrast to MS, where the slopes were less distinctive. In general, the attraction of SPION entrapped in the cells and the magnetic field of MS did not overcome the cells wash-out caused by the flow. Since the strength of the magnetic field presented by MS depends on the inner structure of the steel, it cannot be increased even by the use of a very strong magnet for magnetisation. In this case, in future works, the roughness of the MS and SS should be unified to prevent any fluctuation of cellular attachment.

The flow rate of 10 dynes/cm² applied for the flow experiment represents the arterial range of shear stress within the human body [17]. The flow speed employed in this study was equivalent to the aforementioned parameters. In actual clinical scenarios, SPION-laden HUVECs can be harvested from patients, cultivated, loaded with SPION, and subsequently injected into the circulatory system and captured on the surface of a metal implant, such as a stent. The rationale behind this experimental approach was to emulate the natural flow of blood vessels to assess the feasibility of capturing SPION-laden HUVEC under these conditions. The issue of roughness was encountered, and further research is currently underway to investigate the matter.

Conclusions

This study investigated the attraction of HUVEC to magnetic stainless steel (MS) surfaces mediated by superparamagnetic iron oxide nanoparticles (SPION). The results demonstrated that MS surfaces facilitated enhanced HUVEC adhesion and focal adhesion point formation compared to non-magnetic stainless steel (SS) and SS with an external neodymium magnet. These findings highlight the potential of using magnetic fields generated by MS to improve the initial adhesion of endothelial cells, which is a crucial factor in implant integration and function.

Profilometric analysis revealed that MS surfaces exhibited sharper topographical features than SS, which influenced cellular adhesion. Despite these surface irregularities, SPION-loaded HUVECs under static culture conditions displayed superior attraction to MS surfaces and good spreading, overcoming the restrictive effects of surface roughness. Analysis of cell adhesion and morphology revealed that the presence of SPION significantly influenced endothelial cell behaviour. Quantitative image analysis demonstrated that MS surfaces attracted the highest number of adherent SPION-loaded HUVECs, with statistical significance observed at multiple time points. Furthermore, the circularity of SPION-loaded cells was greatest on MS, indicating that the magnetic interaction counteracted the restrictive effect of sharp surface features, thereby promoting a favourable cellular morphology.

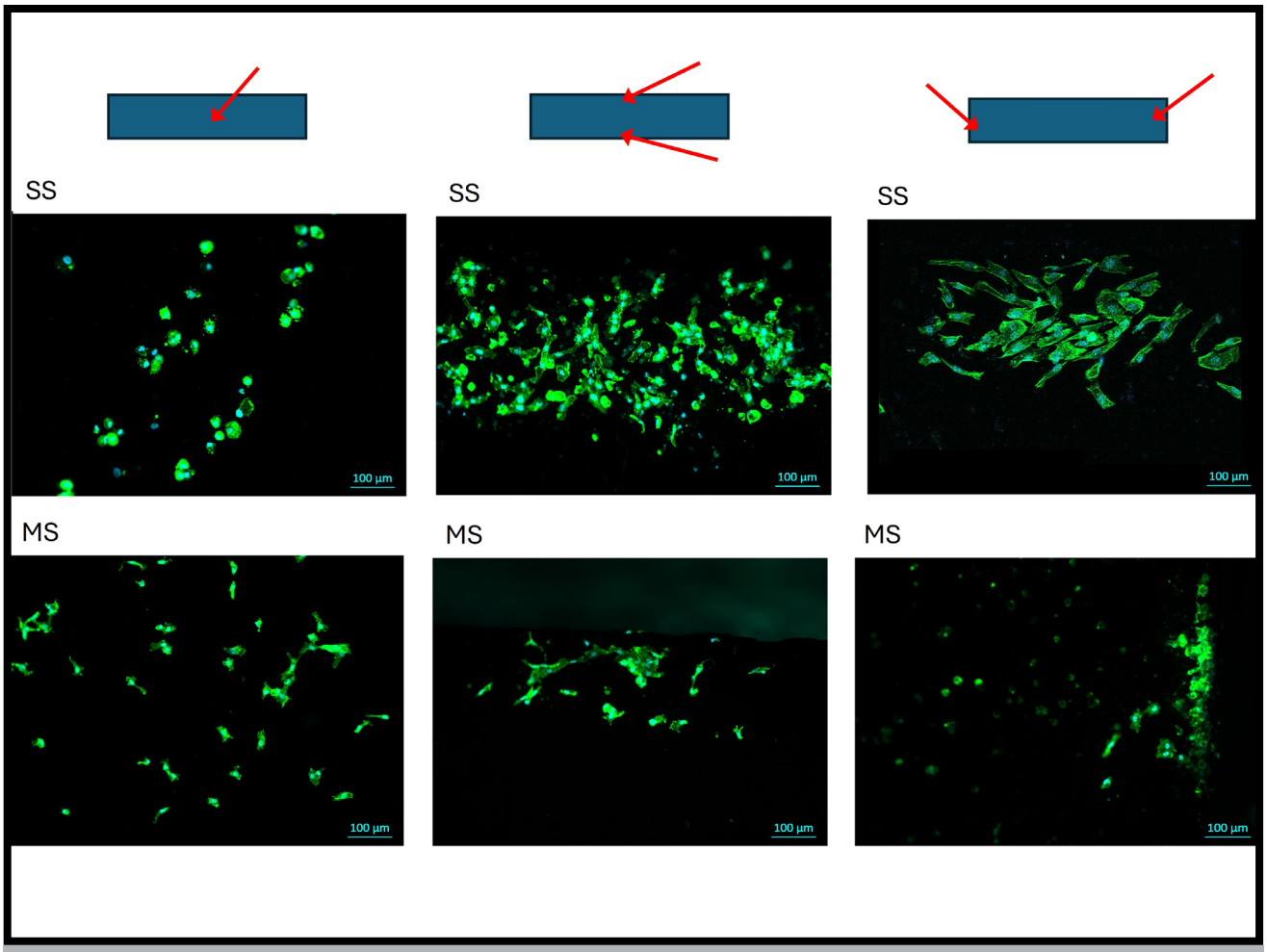

FIG. 9. SPION-loaded HUVECs attached to SS and MS after 20 h of flow culture on different locations of the samples, green – actin, blue – nuclei.

Under static culture conditions, MS surfaces facilitated stronger focal adhesion formation, as evidenced by the distinct clustering of focal adhesion kinase (FAK) at actin filament extremities. This suggests that the magnetic field associated with MS enhances cytoskeletal remodelling and adhesion strength. However, under flow conditions, the benefits of MS surfaces in retaining endothelial cells were limited, as the surface topography was insufficient to prevent cell detachment. This limitation underscores the need for further optimization of surface topography and magnetic properties to enhance endothelial retention in dynamic environments.

In general, this study provides novel insights into the potential of SPION-mediated endothelialization of magnetic stainless steel implants. The findings suggest that weak magnetic fields can improve initial endothelial adhesion and cytoskeletal remodelling, which are critical for implant integration. However, further research is required to enhance endothelial retention under physiological flow conditions. Future studies should focus on optimizing MS surface roughness and exploring alternative strategies to strengthen endothelial cell attachment in dynamic environments. These advancements will contribute to the development of next-generation vascular implants with improved biocompatibility and long-term performance.

Acknowledgements

The research was, in part, founded by the Warsaw University of Technology within the Excellence Initiative: Research University (IDUB) programme, YOUNG PW II activity (agreement no. CPR-IDUB/42/Z01/2024) and Mobility PW V activity.

References

[1] Sigwart U., Puel J., Mirkovitch V., Joffre F., Kappenberger L.: Intravascular stents to prevent occlusion and restenosis after translu minal angioplasty. New England Journal of Medicine 316(12) (1987) 701-706.
[2] Al Suwaidi J., Berger P.B., Holmes D.R. Jr.: Coronary artery stents. Journal of the American Medical Association (JAMA) 284(14) (2000) 1828-1836.
[3] Navarro L., Luna J., Rintoul I.: Surface Conditioning of Cardiovascular 316L Stainless Steel Stents: a Review. Surface Review and Letters 24(01) (2017) 1730002.
[4] Koźlik M., Harpula J., Chuchra P.J., Nowak M., Wojakowski W., Gąsior P.: Drug-Eluting Stents: Technical and Clinical Progress. Biomimetics 8(1) (2023) 72.
[5] Ceylan H., Tekinay A.B., Guler M.O.: Selective adhesion and growth of vascular endothelial cells on bioactive peptide nanofiber functionalized stainless steel surface. Biomaterials 32(34) (2011) 8797-8805.
[6] Ravindranath R.R., De La Franier B., Yougbare I., Fish J.E., Thompson M.: Antibody-Based Capture and Behaviour of Endothelial Cell Lines on Pre-Surface Modified Medical Grade Steel. Recent Progress in Materials 2 (2020) 1-15.
[7] Min Y., Yuan Y., Changsheng L., Jing W.: Development of mussel adhesive polypeptide mimics coating for in-situ inducing re-endothelialization of intravascular stent devices. Biomaterials 30(14) (2009) 2764-2773.
[8] You F., Wu X., Chen X.: 3D Printing of Porous Alginate/gelatin Hydrogel Scaffolds and Their Mechanical Property Characterization. Journal International Journal of Polymeric Materials and Polymeric Biomaterials 66(6) (2016) 299-306.
[9] Polyak B., Fishbein I., Chorny M., Alferiev I., Williams D.N., Yellen B., Friedman G., Levy R.: High field gradient targeting of magnetic nanoparticle-loaded endothel ial cells to the surfaces of steel stents. Proceedings of the National Academy of Sciences of the United States of America 105(2) (2008) 698-703.
[10] Cheng W., Zeng X., Chen H., Li Z., Zeng W., Mei L., Zhao Y.: Versatile Polydopamine Platforms: Synthesis and Promising Applications for Surface Modification and Advanced Nanomedicine. ACS Nano 13(8) (2019) 8537-8565.
[11] Singh R., Wieser A., Reakasame S., Detsch R., Dietel B., Alexiou C., Boccaccini A.R., Cicha, I.: Cell specificity of magnetic cell seeding approach to hydrogel colonization. Journal of Biomedical Materials Research - Part A 105(11) (2017) 2948-2957.
[12] Matuszak J., Zaloga J., Friedrich R.P., Lyer S., Nowak J., Odenbach S., Alexiou C., Cicha I.: Endothelial biocompatibility and accumulation of SPION under flow conditions. Journal of Magnetism and Magnetic Materials 380 (2015) 20-26.
[13] Lutter C., Nothhaft M., Rzany A., Garlichs C.D., Cicha I.: Effect of specific surface microstructures on substrate endothelialisation and thrombogenicity: Importance for stent design. Clinical Hemorheology and Microcirculation 59(3) (2015) 219-233.
[14] Legerstee K., Houtsmuller A.B.: A layered view on focal adhesions. Biology 10 (2021) 11.
[15] Shav D., Gotlieb R., Zaretsky U., Elad D., Einav S.: Wall shear stress effects on endothelial-endothelial and endothelial-smooth muscle cell interactions in tissue engineered models of the vascular wall. PLoS ONE 9 (2014) 2.
[16] Sanchez A.M., Flamini M.I., Zullino S., Gopal S., Genazzani A.R., Simoncini T.: Estrogen receptor-α promotes endothelial cell motility through focal adhesion kinase. Molecular Human Reproduction 17(4) (2011) 219-226.
[17] Cicha I., Beronov K., Ramirez E.L., Osterode K., Goppelt-Struebe M., Raaz D., Yilmaz A., Daniel W.G., Garlichs C.D.: Shear stress preconditioning modulates endothelial susceptibility to circulating TNF-α and monocytic cell recruitment in a simplified model of arterial bifurcations. Atherosclerosis 207(1) (2009) 93-102.